

# Environmental DNA monitoring of pelagic fish fauna at the Hywind Scotland floating wind energy installation – A pilot study

**Authors:**

Jessica Louise Ray, Jon Thomassen Hestetun, Sigrid Mugu, Thomas G. Dahlgren

**Report** 10-2022, NORCE Climate and Environment



Report title	Environmental DNA monitoring of epipelagic fish fauna at the Hywind Scotland floating wind energy installation – A pilot study
Project No	4503971506
Institution	NORCE Climate and Environment
Client	Equinor ASA
Classification:	Open
Report No.	10-2022
No. of pages	34
Date of publ.:	November, 2022
CC-licence	CC-BY-SA
Citation	Ray J., Thomassen Hestetun J., Mugu S., T.G. Dahlgren. 2022. Environmental DNA monitoring of pelagic fish fauna at the Hywind Scotland floating wind energy installation – A pilot study. NORCE report 10-2022.
ISBN	978-82-8408-257-8
Photo Credit	Jessica Ray
Geographical area	United Kingdom, Scotland, Peterhead
Keywords	Hywind, OWF, offshore wind, eDNA, MiFish, ddPCR, metabarcoding, marine environmental monitoring

## Disclaimer

NORCE is not liable in any form or manner for the actual use of the documents, software or other results made available for or resulting from a project and does not warrant or assume any liability or responsibility for the completeness or usefulness of any information unless specifically agreed otherwise in the tender and resulting contract document.

## Summary

Environmental impact assessment and regular environmental monitoring are prerequisites for the construction, operation, and decommissioning of offshore installations such as the Hywind Scotland wind park. Molecular approaches are increasingly being considered as a possible complement or alternative to currently used marine baseline and monitoring methods, both for pelagic and benthic organism studies. The following report is a proof-of-concept study where two molecular methods, metabarcoding and quantitative assays, have been used to characterize the pelagic environment at the Hywind Scotland wind park based on filtered water samples from the installation and a reference area. The purpose of the report is to showcase the use of molecular methodology in future studies of the pelagic ecosystem. Metabarcoding was employed for a community view of a) fish species specifically, using the MiFish primer set, and b) a universal eukaryote dataset based on 18S V1-V2 primers. Quantitative assays were employed for two commercially important pelagic fish species: mackerel and herring.

MiFish results comprised the detection of 39 fish species. Atlantic mackerel, sprat, Atlantic herring, haddock, pouting, and lemon sole were the most abundant in terms of sequence reads. Mackerel abundance was higher at 10 m depth compared to 50 m, equally distributed in installation and reference areas, for sprat and herring, abundance was high at both 10 m and 50 m, with higher abundance in the installation. The 18S data were dominated by alveolates, then metazoans, where copepods represented most reads. Beta diversity analysis of both MiFish and 18S data showed a clear and significant separation in data according to depth. For the fish specific MyFish marker the signals for typical pelagic species were consistently stronger at 10 m while demersal species had a stronger signal at the 50 m depth. A small but less clear difference in diversity data were also found between the installation and reference areas, but in the case of e.g., pelagic fish composition and their relative abundance, this difference could also be dependent on random placement of schools at the time of sampling. Sampling over a longer time frame than one day would strengthen any conclusions regarding these differences. The results show that metabarcoding has high potential to be used as an environmental monitoring method for the pelagic ecosystem and validate the ability of metabarcoding data to reflect differences in underlying organism community composition.

The test of the quantitative assays for mackerel and herring showed clearly that they worked with no indication of unspecific amplification (false positives). The results were further corroborated by the number of reads in the metabarcoding dataset. In the park area, there were significant differences in the signal from the two depths for mackerel with a higher biomass of mackerel at the 10 m depth compared to the 50 m depth. There was also an indication of higher biomass of mackerel at 10 m depth in the reference area. There was no significant difference in biomass of mackerel between the installation and the reference area when considering both sampling depths combined.

The data for herring showed a slightly different pattern with a significantly higher biomass in the installation compared to the reference area, but also for this species, there were indications of higher biomass in the 10 m samples than in the 50 m samples, especially in the reference area.

We conclude that ddPCR using species specific assays applied on water samples is a powerful tool to assess biomass of pelagic species using filtered samples of water. To account for temporal and spatial variation in the behavior of these species, a full-scale project would benefit from samples taken at night and samples taken during other seasons. The statistical power would also benefit for samples taken over more days than what was possible here (one day only). In that way any coincidence in the distributions of shoals that may have contributed to the indicated increased biomass of herring in the installation would be ruled out. In this pilot project we included a reference area at a distant of 10 km away from the installation in a direction perpendicular to the current. To better understand the degradation of DNA over time samples also in the direction of the current could be considered. One major benefit of eDNA sampling is the restricted use of pelagic trawl inside an offshore wind farm. To better understand the correlation between eDNA results and actual fish biomass, eDNA samples should be taken and trawling conducted simultaneously in the same area. One could consider trawling to be conducted in the reference area that would allow for a ground proofing of the data also in a near-by installation.

## Table of contents

1.	Introduction .....	5
2.	Materials and methods.....	7
2.1.	Study area.....	7
2.2.	Field sampling.....	8
2.3.	Lab processing.....	10
2.4.	Droplet digital PCR analysis.....	11
2.5.	Metabarcoding .....	11
3.	Results.....	13
3.1.	Droplet digital PCR results.....	13
3.2.	MiFish metabarcoding results.....	17
3.3.	18S rRNA metabarcoding results .....	21
4.	Discussion and Conclusions .....	25
4.1.	Droplet digital PCR .....	25
4.2.	Metabarcoding .....	26
5.	References .....	29
	Appendix A: MiFish sequence read abundances .....	0

## 1. Introduction

The Hywind Scotland Pilot Project is a floating offshore wind farm (OWF) situated at the Buchan Deep, east of Peterhead, UK (Fig. 1). As part of the operation of the OWF, environmental impact assessments, baseline and monitoring surveys cover various aspects of the construction, operation, and decommissioning. To complement existing monitoring studies, NORCE was contracted to conduct environmental DNA monitoring of water samples from the OWF, with an emphasis on detection of and potential impact on commercially important pelagic fish species. Pelagic species are notoriously difficult to monitor in OWFs and data on any impact is scarce. The molecular monitoring in this report is designed as a proof-of-concept study to assess the viability of routine implementation of similar future studies pending regulatory acceptance.

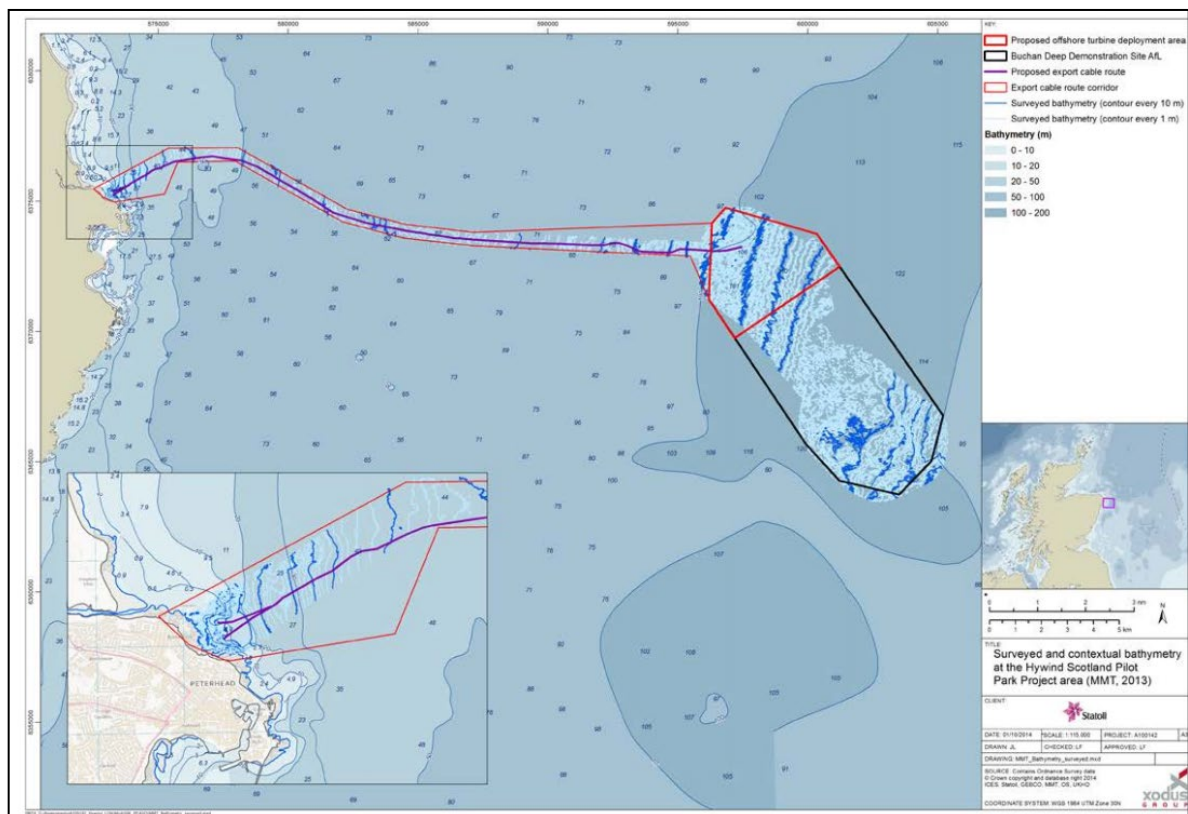


Figure 1. Map of the Hywind Scotland Pilot Project wind farm area. Source: Hywind Scotland Pilot Park Environmental Statement.

Fishing activities are prohibited in most OWF during operation of the installations and that have been shown to have a strong positive impact on abundance and diversity of the demersal fish assemblage (Bergström et al. 2013). Fishing at HyWind Scotland OWF is allowed but is believed to be limited to use of passive gear since trawls are difficult to operate in between the turbines with their anchors. The main drivers for the positive effects are the increase in habitat heterogeneity, the reef effect and the removal of the bottom trawling from the area (e.g. Bergström et al. 2014, Stenberg et al. 2015). Based on this, OWF has been suggested to act as marine protected areas in coastal zone management practices (Inger et al. 2009). The pelagic fish community is normally assessed using pelagic trawls in combination with sonar and because of the restrictions on use of trawls, is more difficult to monitor in an OWF and there are thus less studies available that have successfully measured any impact (Methratta 2021). Recent research, however, compared eDNA

based data with trawl and sonar data showing a strong correlation and concluded that eDNA based methods are a good proxy for fish assessments (Stoeckle et al. 2021, Shelton et al. 2022).

What the main mechanisms would be that may have an impact on pelagic fish species are not well understood. The Fish Aggregating Device (FAD) effect got its name from fisherman most often in the open ocean tropics environments noticing that pelagic fish species gathered close to large floating object and started to use them for easier catch (Dempster and Taquet 2004). Although not very well covered in the scientific literature, it has been shown that pelagic fish gather at other types of artificial structures in the ocean (e.g. Munnely et al. 2021). OWF turbine foundations has also been shown to attract fish that may alter the abundance of pelagic species.

Other possible effects that may impact the pelagic fish fauna relates to how the OWF may alter open ocean circulation leading to changes in eg primary production. This change could potentially impact zooplankton abundance and hence pelagic food availability in the general area of the OWF that in turn could impact the pelagic fish fauna.

The altered upper ocean circulations have two general sources (i) changes caused by a shift in wind patterns caused by the turbines (Broström 2008); and (ii) changes in turbulence from the turbine foundations inside the OWF (Sumer and Fredsøe 1997). A recent report suggested that the combined effect from these processes can be significant (van Berkel et al. 2020). The larger primary production can possibly be compensated by a larger abundance of filter feeders which may remove some of that production from the water mass and deposit it on the seafloor (Slavik et al. 2019, Ivanov et al. 2021).

The primary goal of this pilot study is to assess the use of eDNA for monitoring of the pelagic fish fauna in OWF. For this purpose, we use two types of analyses: (i) metabarcoding to assess the diversity of the fauna, and (ii) droplet digital PCR (ddPCR) to estimate the abundances of two specific target species.

## 2. Materials and methods

### 2.1. Study area

The Hywind Scotland floating OWF was opened for operation in 2017 and is located 25 km east of Peterhead at the Buchan Deep. It is composed of five floating turbine units with a hub height of 82-101 m and rotor diameter of 154 m, placed 800-1600 m apart, each moored by three anchors with 600-1200 m mooring radius, and is further connected by 33 kV inter-array cables connected to the Peterhead Grange Substation. The following information is adapted from the Hywind Scotland Environmental Statement (Statoil 2015).

The water depth is 100-120 in the OWF area, with wave direction predominantly from the north and currents dominated by tides moving in a north south pattern sometimes at a significant speed. Bottom conditions are a blend of sand and gravel with scattered boulders (defined as “circalittoral fine sand”), no significant contamination levels measured, with megafauna including sparse hermit crabs, brittle stars (*Ophiura* sp.), hydroids and anemones on the scattered hard substrate. Main infaunal species include polychaetes *Scoloplos armiger*, *Spiophanes bombyx* and *Owenia fusiformis* and echinoderms *Ophiura affinis*, *Amphiura filiformis*, *Echinocyamus pusillus* and *Spatangus* sp.

Peterhead is the largest commercial fishing port in the UK, and 72% of Peterhead vessels and 47% of nearby Fraserburgh vessels have fished in the wider area around the wind park.

**Table 1.** Planned positions for the stations sampled at HyWind Scotland (IA1-5) and in the reference area (RA1-5).

Station Name	Latitude	Longitude
IA1	57° 29.063'N	01° 22.837'W
IA2	57° 29.620'N	01° 22.122'W
IA3	57° 28.712'N	01° 21.536'W
IA4	57° 29.103'N	01° 20.795'W
IA5	57° 29.323'N	01° 19.951'W
RA1	57° 29.216'N	01° 12.828'W
RA2	57° 29.907'N	01° 11.981'W
RA3	57° 28.712'N	01° 11.621'W
RA4	57° 29.103'N	01° 10.496'W
RA5	57° 29.323'N	01° 09.601'W

The area contains typical North Sea fish stocks. Pelagic fishes include Atlantic herring (*Clupea harengus*), and mackerel (*Scomber scombrus*), which are commercially exploited in the area, and sprat (*Sprattus sprattus*). Demersal species include cod, haddock, whiting, plaice, lemon sole, anglerfish ling, European hake, Norway pout, saithe, spotted ray, common skate, spurdog and tope. The area is also a spawning ground for sandeel, cod, whiting, plaice and European lobster, and a nursery ground for sandeel, cod, haddock, whiting, lemon, sole, anglerfish, ling, European hake, spurdog, tope, common skate, spotted ray and saithe. The area is expected to act as a transit area for diadromous species such as Atlantic salmon, sea trout, European eel, river lamprey and sea lamprey.



## 2.2. Field sampling

A sampling cruise was conducted on board the MCS Swath 1 on 10 August 2021. A 10 x 8 ft (3.05 x 2.44 m) metal container with wall-mounted table, electricity and ceiling lighting was lifted onto deck and rigged as a makeshift onboard “laboratory” for filtering of water samples immediately after collection. To identify if any stratification was present in the water column, CTD profiles were taken at all sampling sites in both the impact and reference areas (Fig. 2). No significant stratification was observed, so it was decided to collect water samples at both 10 m and 50 m depth at all ten sampling stations as planned (Table 1). These two depths were considered as representative for the water masses present in the area. Two CTD profiles down to 50 m with GPS coordinates were taken at each station and used to correct vessel drift relative to planned sampling stations (Table 1; Fig. 3).

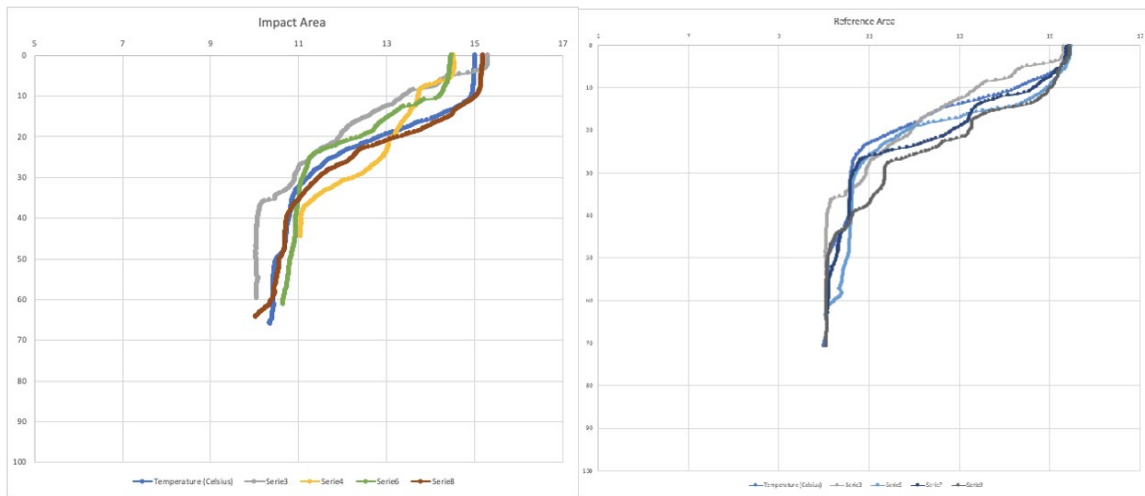


**Figure 2.** Hywind Scotland. CTD profiles at each of the sampled stations in the OWF Impact area and Reference area.

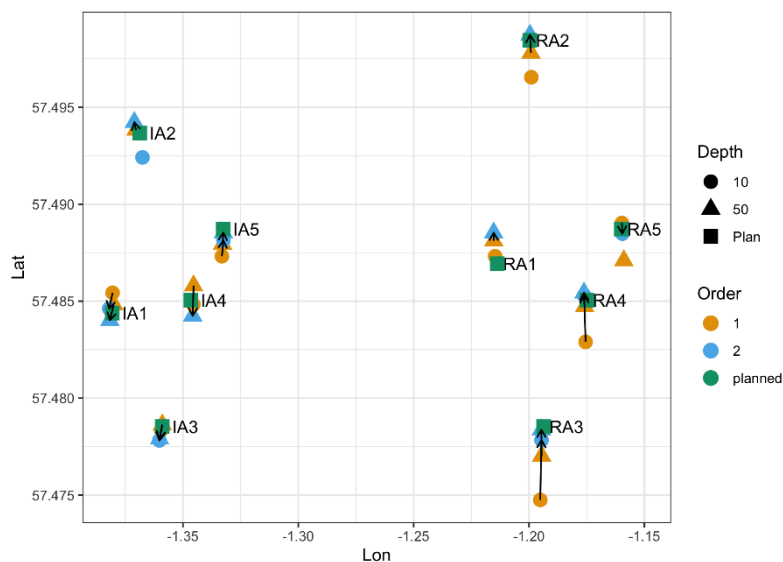


**Figure 3.** Two-dimensional plot of planned sampling stations (green squares) and actual sampling stations (yellow and blue symbols) for the Hywind Scotland eDNA pilot study. GPS coordinates were recorded at the start (yellow symbols) and finish (blue symbols) of each water sampling deployment

(10 m, circles; 50 m, triangles) so that ship drift during sampling (arrows) could be recorded and corrected as necessary.

Equipment and working surfaces were decontaminated with 5% (v/v) sodium hypochlorite, sodium hydroxide solution (household bleach) prior to commencement of work and between sampling stations to reduce ambient and carryover eDNA contamination. Water was collected using a weighted 5L-Niskin bottle deployed individually on a manual winch and closed at desired sampling depth using metal messengers deployed from deck. The contents of each Niskin bottle were dispensed into three - 1L brown polypropylene bottles that had been thrice rinsed with sample water prior to filling. These triplicate water subsamples were filtered in parallel through 0.45  $\mu\text{m}$  Sterivex PES filters using Masterflex peristaltic pump with a four-channel pump head and pumping speed of 300 rpm. Subsamples from 10 m and 50 m depth were filtered simultaneously using a mirrored pump set-up to maximize throughput at each sampling station (Fig. 4).



**Figure 4.** Simultaneous filtration of collected water samples inside the on-deck container using peristaltic pumps powered from electricity to the container. Triplicate 1L-water samples (brown bottles) from each sampling depth (50 m on the left, 10 m on the right) were filtered through 0.45  $\mu\text{m}$  Sterivex filters using four-channel pump heads set to 300 rpm (flow rate approx. 100 mL min<sup>-1</sup>). Filter outflow was collected in 2L-beakers, and outflow volume was measured and recorded.

Pump tubing was decontaminated between water samples by filling with 5% (v/v) bleach solution, allowing to stand for 5 minutes, emptying, flushing with 200 mL distilled water, allowing to stand while filled with distilled water for 5 minutes, emptying, and then flushing with approx. 100 mL of the next water sample prior to filter attachment and sample filtration. Filtering speed for all samples was approximately 100 mL min<sup>-1</sup>. Outflow volume from each filter was recorded. Excess water was expelled from filters using a 60 mL syringe filled with 0.22  $\mu\text{m}$  sterile-filtered air. Air and water blank samples were also collected at each station to control for ambient and carry-over contamination, respectively. Air blanks consisted of pressing non-sterile-filtered air from a 60 mL syringe into a 0.45  $\mu\text{m}$  Sterivex PES filter. Water blanks were prepared by filtering 1 L of distilled water (the same water used for rinsing pump tubing) through a 0.45  $\mu\text{m}$  Sterivex PES filter. Finally, all filters were filled with

Buffer ATL (QIAGEN) as preservative (Majaneva et al. 2018), capped, placed individually inside sterile 50 mL polypropylene tubes, and stored cool and dark until transport back to Bergen on 11 August 2021. Upon arrival in Bergen, filters were stored at -20°C until eDNA extraction.

### 2.3. Lab processing

Lysis of filtered particles was conducted inside Sterivex filters to minimize contamination and maximize lysis efficiency. Sixty microliters of 20 mg mL<sup>-1</sup> Proteinase K (QIAGEN) were added to each thawed filter containing Buffer ATL preservative. Filters were tightly capped and incubated at 56°C with gentle rotation overnight. Lysate was aspirated from Sterivex filters using sterile 5 mL syringes and lysate volume was recorded. One millilitre of each lysate was taken for DNA purification while the remaining lysate was archived at -80°C. DNA purification was conducted using the DNeasy Blood & Tissue kit (QIAGEN) according to the manufacturer's protocol, with two modifications: (1) Added volumes of RNase A (100 mg mL<sup>-1</sup>) and Buffer AL were adjusted to compensate for increased starting volume of lysate; (2) Buffer AL-treated lysates were applied to silica spin columns in multiple centrifugation rounds to allow binding of the entire lysate volume. Purified DNA was eluted in 200 µL Buffer EB (QIAGEN) and divided into one archive aliquot (-80°C storage) and one working aliquot (-20°C storage).

**Table 2. Primers and probes used in the study.** References for all primer and probe sequences can be found in Section 2.4 and 2.5 of the Materials & Methods.

Oligo name	5'-3' DNA sequence	Final conc.	Function
<b>ddPCR <i>Scomber scombrus</i> (Atlantic mackerel)</b>			
Scosco_CYBF14517	TTCCCTGCTTGGTCTCTGTT	400 nM	forward primer
Scosco_CYBR14597	GGCGACTGAGTTGAATGCTG	800 nM	reverse primer
Scosco_CYBP14541*	TTCCCAAATCCTCACAGGACTATTC	200 nM	probe
<b>ddPCR <i>Clupea harengus</i> (Atlantic herring)</b>			
Cluhar_CYBF14928	CCCATTGTGATTGCAGGGG	200nM	forward primer
Cluhar_CYBR15013	CTGAGTTAAGTCTGCCGGG	1000 nM	reverse primer
Cluhar_CYBP14949*	TACTATTCTCCACCTTCTGTTCTC	200 nM	probe
<b>Metabarcoding 18S (V1-V2) ribosomal RNA gene</b>			
SSU_F04mod	GCTTGWCTCAAAGATTAAGCC	240 nM	forward primer
SSU_R22	CCTGCTGCCTTCCTTRGA	240 nM	reverse primer
<b>Metabarcoding MiFish</b>			
MiFish-U-F	GTCGGTAAACTCGTGCCAGC	300 nM	forward primer
MiFish-U-R	CATAGTGGGGTATCTAATCCCAGTTTG	300 nM	reverse primer

\* ddPCR probes were modified at the 5'-end with the 6-FAM fluorophore and at the 3'-end with the BHQ1 fluorescence quencher

## 2.4. Droplet digital PCR analysis

Quantitative molecular detection was conducted using a DX200 droplet digital PCR (ddPCR) system (Bio-Rad) with published assays targeting the mitochondrial cytochrome B gene (*cytB*) of either Atlantic mackerel (*Scomber scombrus*) or Atlantic herring (*Clupea harengus*) (Knudsen et al. 2019) (Table 2). ddPCR master mixes were prepared in a template-free pre-PCR laboratory room inside a class II biosafety cabinet with laminar air flow using UV-treated plastics. Template DNA was added to pre-prepared ddPCR master mixes while working inside a second, class II biosafety cabinet inside a separate lab purposed for DNA/RNA work. Both labs have positive pressure HEPA-filtered ventilation to reduce exterior airborne contamination.

For Atlantic mackerel, triplicate 20  $\mu$ L ddPCR assays consisted of (final concentration) 400 nM forward primer Scosco\_CYBF14517 (5'-TTCCCTGCTTGGTCTCTGTT-3'), 800 nM reverse primer Scosco\_CYBR14597 (5'-GGCGACTGAGTTGAATGCTG-3'), 200 nM probe Scosco\_CYBP14541 (5'-[FAM]TTCCCAAATCCTCACAGGACTATTC[BHQ1]-3'), 1X ddPCR Supermix for probes (Bio-Rad) and 5  $\mu$ L undiluted template. The PCR amplification program for herring consisted of an initial denaturation at 95°C for 10 min, followed by 45 cycles of 94°C for 30 sec and 54 °C for 60 sec, and a final denaturation at 98°C for 10 min.

For Atlantic herring, triplicate 20  $\mu$ L ddPCR assays per sample consisted of (final concentration) 200 nM forward primer Cluhar\_CYBF14928 (5'-CCCATTGTGATTGCAGGGG-3'), 1000 nM reverse primer Cluhar\_CYBR15013 (5'-CTGAGTTAAGTCCTGCCGGG-3'), 200 nM probe Cluhar\_CYBP14949 (5'-[FAM]TACTATTCTCCACCTTCTGTTCTC[BHQ1]-3'), 1X ddPCR Supermix for probes (Bio-Rad), and 5  $\mu$ L undiluted template. Ultrapure water was added instead of template DNA for ddPCR negative (no template) controls. PCR reactions were emulsified using a droplet generator (Bio-Rad) according to manufacturer instructions. The PCR amplification program for mackerel consisted of an initial denaturation at 95°C for 10 min, followed by 40 cycles of 94°C for 30 sec and 59°C for 60 sec, and a final denaturation at 98°C for 10 min.

After a brief equilibration to room temperature, droplet fluorescence was read using a droplet reader (Bio-Rad) with default settings for FAM detection. Absolute target gene copies per microliter in ddPCR reactions were normalized to copies L<sup>-1</sup> seawater.

Statistical analysis and visualization of ddPCR results were conducted in the R statistical computing environment (R Core Team, 2021). GPS coordinates were converted from decimal degrees to decimal using the `parzer::parse_lon()` and `parzer::parse_lat()` commands (Chamberlain and Sagouis 2021). Mean GPS positions at each sampling station were calculated using the `stats::aggregate()` function. Data visualization was done using the `base` (R Core Team, 2021) and `ggplot2` (Wickham, 2016) packages. Single-factor (area or depth) explanatory power on ddPCR results (copies L<sup>-1</sup>) was tested using `stats::kruskal.test()` with default parameters.

## 2.5. Metabarcoding

Two complementary primer pairs were chosen for metabarcoding amplification: The MiFish universal fish 12S rRNA gene primer pair MiFish-U-F (5'-GTCGGTAAACTCGTGCCAGC-3') and MiFish-U-R (5'-CATAGTGGGGTATCTAATCCCAGTTTG-3') (Miya et al. 2015), specifically to capture fish communities in the area, and 18S V1-V2 universal eukaryote primers with primers SSU\_F04mod (5'-GCTTGWCTCAAAGATTAAGCC-3') (Cordier pers. comm.) and SSU\_R22 (5'-

CCTGCTGCCTTCCTTRGA-3') (Sinniger et al. 2016), to capture a broad range of eukaryote single-celled and animal diversity (Table 2). PCR amplification was done with adapter-linked primers using the KAPA3G Plant PCR kit (KAPA Biosystems) with annealing temperatures at 65 °C and 57 °C for MiFish and 18S primers respectively. Three (18S) and eight (MiFish) PCR replicates were made for each sample, and subsequently pooled prior to sequencing. Library preparation was done using equimolar pooled PCR product with Illumina dual index TruSeq i5/i7 barcodes. Field sampling, extraction and PCR negative controls were used to detect contamination due to sample processing. Sequencing was performed on an Illumina MiSeq instrument using v3 with 300 bp chemistry at the Norwegian Sequencing Centre (University of Oslo, Norway).

Initial quality check of sequence fastq files was done using FastQC v0.11.8 (Andrews 2010). Cutadapt v1.18 (Martin 2011) and VSEARCH v2.11.1 (Rognes et al. 2016) were used for pairwise merging and filtering, then SWARM v2.2.1 (Mahé et al. 2015) was used to derive OTUs from dataset sequences, with subsequent post-clustering curation using LULU. Taxonomy was assigned using CREST4 with the Silvamod 1.38 database for 18S data, and Sintax assignment using VSEARCH with the MitoFish database (Iwasaki et al. 2013) for the MiFish 12S data.

Multivariate analysis, including Hellinger transformation, Bray-Curtis dissimilarity, non-metric multidimensional scaling (NMDS) and cluster plots, PERMANOVA and SIMPER analyses were done using the R vegan package v 2.5-7 (Oksanen et al. 2020). Data visualization was done using the ggplot2 (Wickham 2016) package.

### 3. Results

#### 3.1. Droplet digital PCR results

In total, we performed 486 ddPCR reactions to quantify eDNA of Atlantic mackerel (*Scomber scombrus*) (N = 243 reactions) and Atlantic herring (*Clupea harengus*) (N = 243 reactions). eDNA signal for mackerel ranged from 0 (non-detected; N = 109 samples) to 1016.4 copies L<sup>-1</sup>, which occurred in a 10 m sample from station IA1 inside the Hywind Scotland wind park (Figure 5A). For herring, ddPCR results ranged from 0 (non-detected; N = 92) to 1026.6 copies L<sup>-1</sup> in a 50 m sample from station IA3 inside the wind park (Fig. 5B). Detection rates for filter eDNA samples were 39% for mackerel (71 positive detections from 180 samples analysed) and 49% (88 positive detections from 180 samples analysed) for herring.

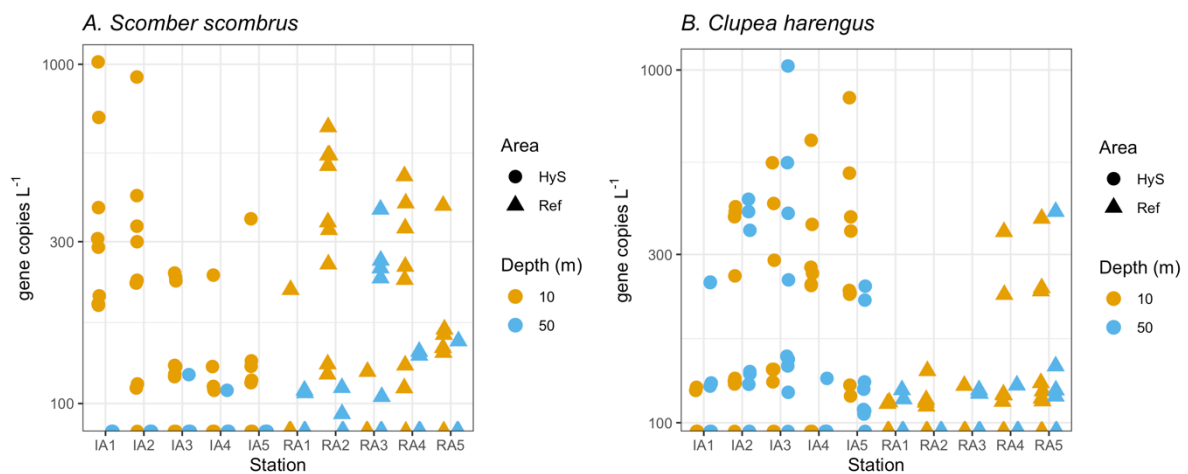


**Figure 5.** Scatterplots showing ddPCR quantification results for (A) Atlantic mackerel (*Scomber scombrus*) and (B) Atlantic herring (*Clupea harengus*) at the ten sampling stations investigated in the pilot study. Station name/number are shown on the x-axis. IA - impact area stations within the Hywind Scotland wind park; RA - reference stations located in a similar size area 10 km to the east of the wind park. ddPCR results (y-axis) are shown as target gene copies per liter of seawater. Circles show results from samples taken inside the wind park. Triangles show results from samples taken in the reference area. Yellow symbols represent samples collected from 10 m sampling depth. Blue symbols represent samples collected from 50 m sampling depth. Samples without detection were arbitrarily set to 0 for plotting purposes and are shown as points lying on the x-axis.

ddPCR quantification revealed that the mackerel eDNA signal inside the wind park was not significantly different from the reference area when the 10 m and 50 m samples were pooled (Fig. 6A). We did, however, observe a significant difference in mackerel eDNA detection between the wind park and reference area when the two sampling depths were considered independently, with higher eDNA detection at 50 m sampling depth in the reference area (Fig. 6B). Non-parametric rank sum tests using mackerel eDNA copies L<sup>-1</sup> as response variable and either area (Kruskal-Wallis chi-squared = 0.0022121, df = 1, p-value = 0.9625) or depth (Kruskal-Wallis chi-squared = 46.886, df = 1, p-value = 7.524e-12) as explanatory variable confirmed these observations.

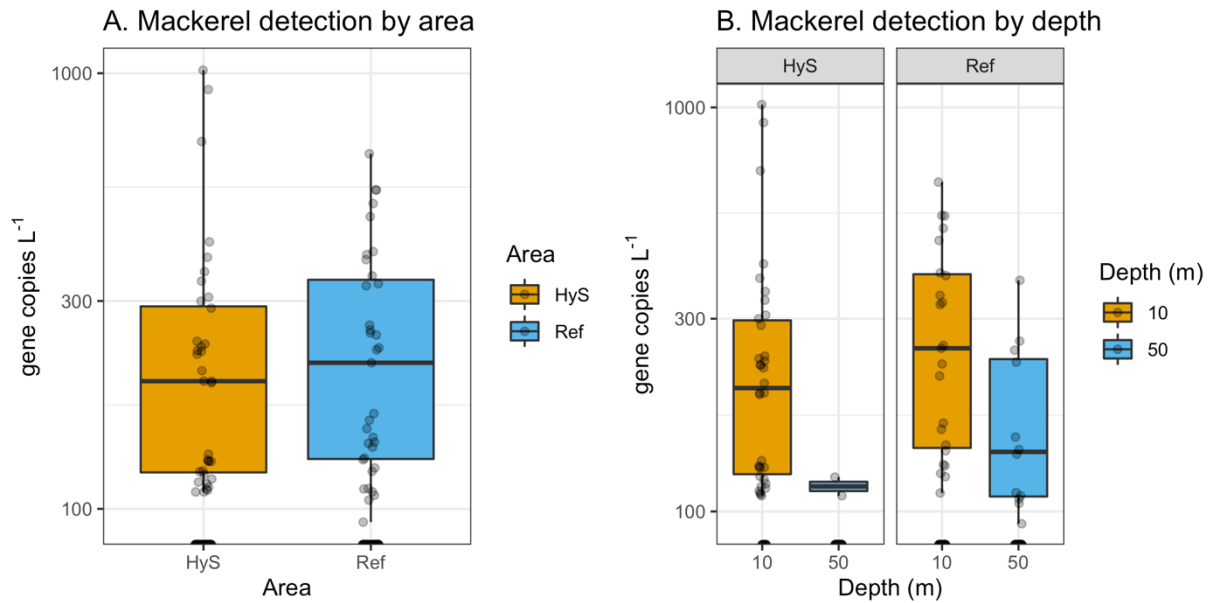


**Figure 6.** Box-and-whisker plots summarizing ddPCR results for Atlantic mackerel (A) between the wind park (HyS, yellow bars) and reference area (Ref, blue bars), and (B) by sampling depth (10 or 50 m). Logarithmic y-axis shows target gene copies per liter of seawater.

We also observed differences in mackerel eDNA detection between sampling stations (Fig. 7A,B versus Fig. 7C,D), with clear differences between sampling depths as well (Fig. 7A,C versus Fig. 7B,D).

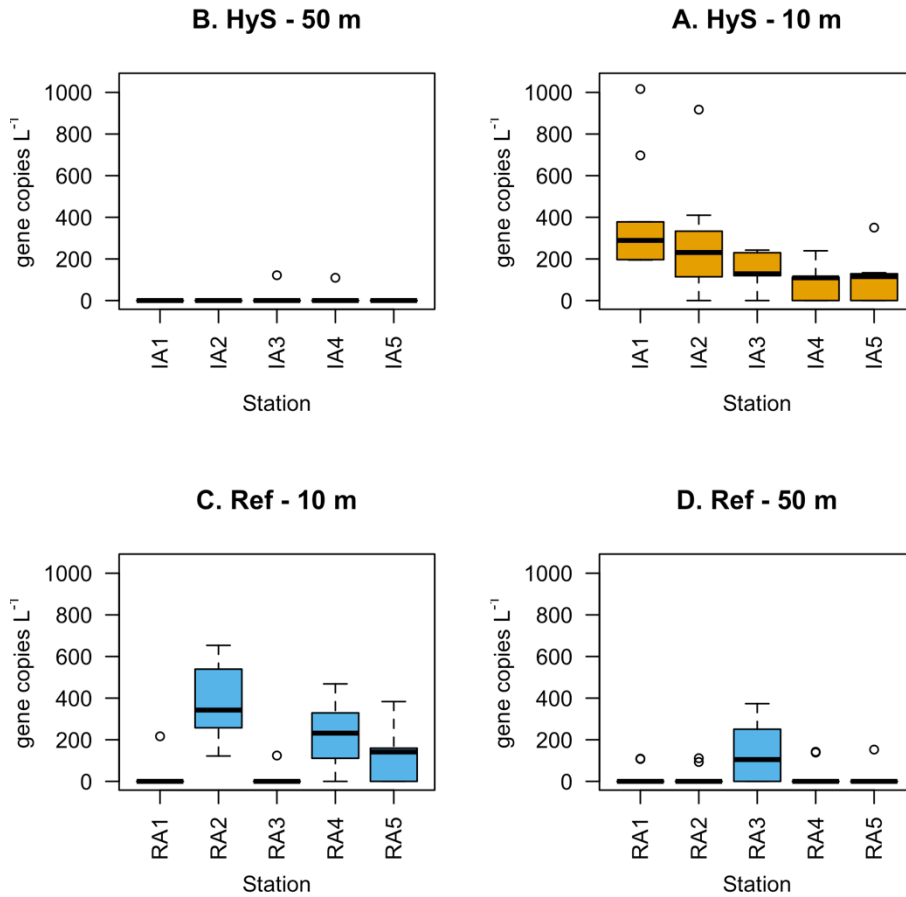


**Figure 7.** Box-and-whisker plots summarizing ddPCR results for Atlantic mackerel by sampling area (A,B - wind park or C, D - reference area), by sampling depth (A, C - 10 m or B, C - 50 m) and by sampling station (IA1-IA5 - wind park; RA1-RA5 - reference area). Non-detections were arbitrarily set to 0 for visualization purposes.

For herring, ddPCR analysis revealed significantly higher herring eDNA detection inside the wind park relative to the reference area (Fig. 8A). We also observed higher detection of herring eDNA at 50 m sampling depth inside the wind park compared to the same depth in the reference area (Fig. 8B), which is in contrast with the depth-dependent detection of mackerel shown above (Fig. 8B). Non-parametric rank sum tests confirmed the significance of both sampling area (Kruskal-Wallis chi-squared = 31.548, df = 1, p-value = 1.946e-08) and depth (Kruskal-Wallis chi-squared = 4.9515, df = 1, p-value = 0.02607) for detection of herring eDNA from filtered water samples.



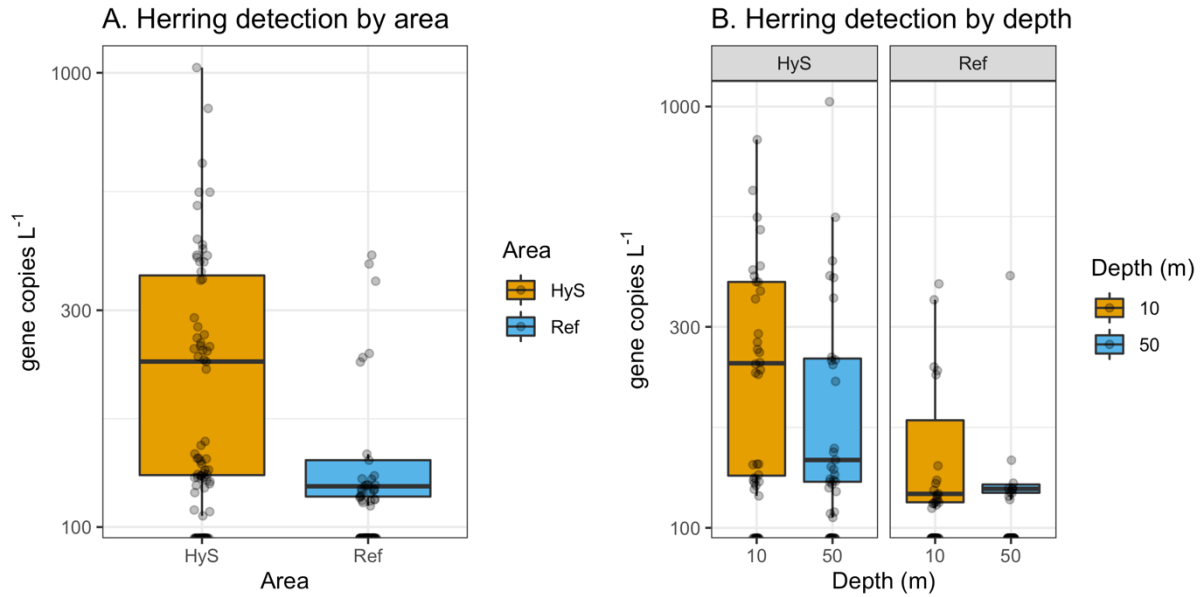


**Figure 8.** Box-and-whisker plots summarizing ddPCR results for Atlantic herring (A) between the wind park (HyS, yellow bars) and reference area (Ref, blue bars), and (B) by sampling depth (10 or 50 m). Logarithmic y-axis shows target gene copies per liter of seawater.

Similar to mackerel, we also observed differences in herring eDNA detection between sampling stations (Fig. 9 A-D).

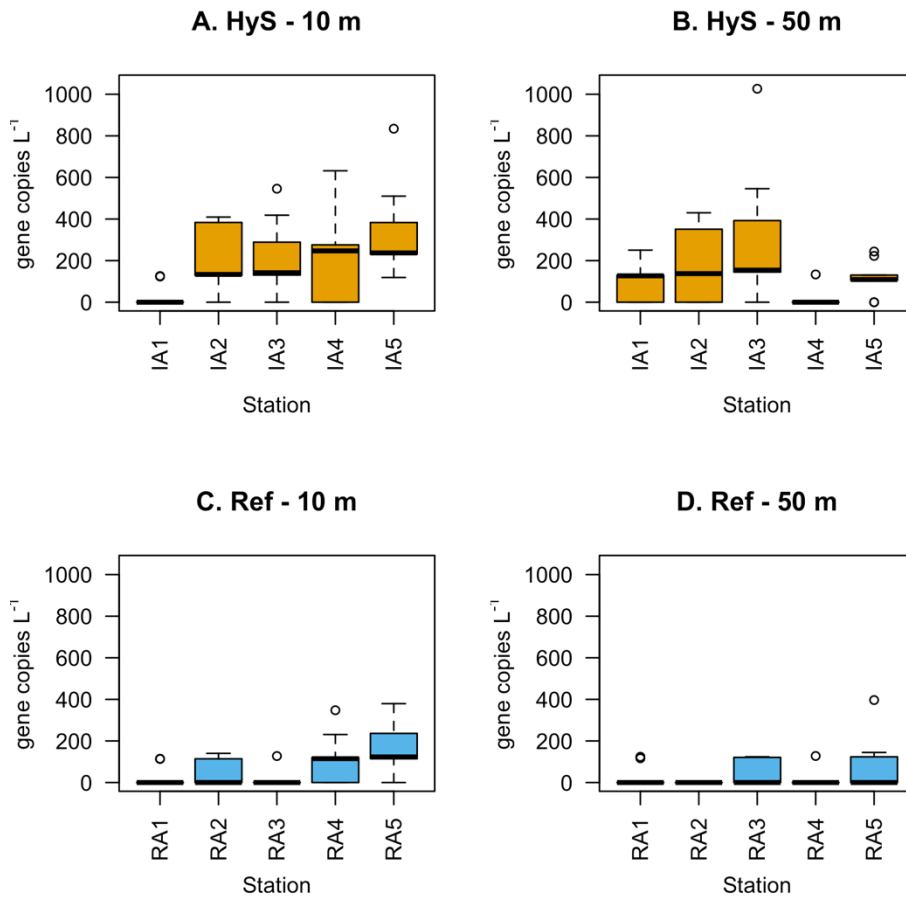


**Figure 9.** Box-and-whisker plots summarizing ddPCR results for Atlantic herring by sampling area (A,B - wind park or C, D - reference area), by sampling depth (A, C - 10 m or B, C - 50 m) and by sampling station (IA1-IA5 - wind park; RA1-RA5 - reference area). Non-detections were arbitrarily set to 0 for visualization purposes.

In addition to eDNA filter samples, 63 control samples from triplicate analysis of 10 air blanks, 10 water blanks, 1 ATL blank, as well as ddPCR negative controls, were analyzed in parallel to eDNA filters samples to control for background eDNA signal. Atlantic mackerel eDNA was not detected in any of the 63 controls samples or ddPCR negative controls. Atlantic herring eDNA, however, was detected in seven technical replicates from control samples: four air blanks (“AB”), two water blanks (“WB”) and one Buffer ATL blank (“ATL”), with values ranging from 4.8 copies L<sup>-1</sup> in the air blank from station IA2 to 255 copies L<sup>-1</sup> in the water blank from station IA5 (Fig. 10). Positive detections in negative control samples were in general anecdotal and appeared in only one of three technical replicates, except for station IA5 where two of three replicates for the water blank gave positive detections (Fig. 10).

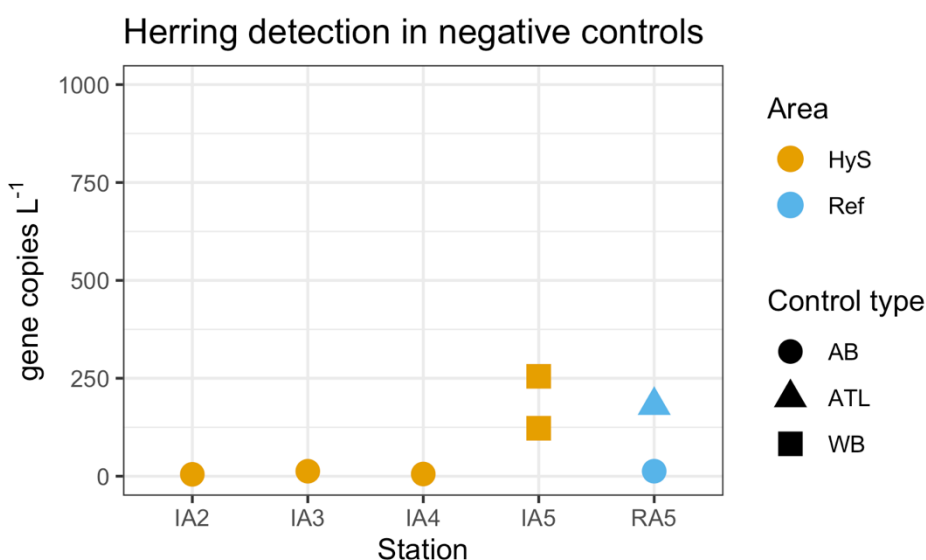


**Figure 10.** Scatterplot showing ddPCR detection of Atlantic herring eDNA in negative control samples. Sampling station at which each sample was collected is indicated on the x-axis (IA2-IA5 - wind park; RA5 - reference area). Yellow symbols show control samples collected inside the wind park. Blue symbols show control samples collected in the reference area. Circles represent air blank (“AB”) controls; squares represent water blank (“WB”) controls; triangle represents preservation buffer (“ATL”) control. Linear y-axis shows target gene copies per liter of control medium (air, water or preservation buffer) filtered.

### 3.2. MiFish metabarcoding results

The total number of raw sequences from the MiFish dataset were 4 176 470 reads from 60 samples (five park and five reference stations, each at 10 and 50 m depth, each with three replicates) and 28 controls, with 5 336-112 708 sequences from individual samples (average: 54 968). After bioinformatic processing and filtering, 4 087 488 sequences remained. After SWARM clustering, 2 312 potential OTUs were identified from sequences in the dataset, with 236 OTUs were retained after chimera filtering and LULU curation. Taxonomic assignment of these OTUs using the MitoFish

database yielded 39 separate fish species, one record of harbor porpoise, and four non-target taxa (cattle, sheep, human, polychaete) (Appendix A).

Atlantic mackerel (*Scomber scombrus*) was the most abundant species, followed by sprat (*Sprattus sprattus*), Atlantic herring (*Clupea harengus*), haddock (*Melanogrammus aeglefinus*), pouting (*Trisopterus luscus*) and lemon sole (*Microstomus kitt*) (Fig. 11; Table 3).

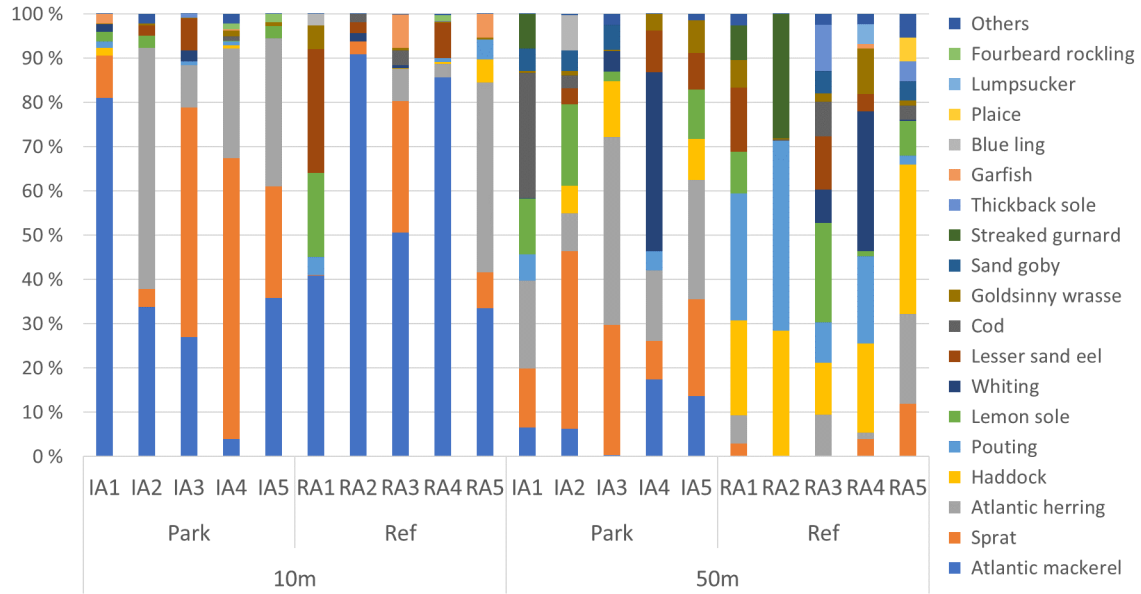


**Figure 11.** Relative abundance of the 18 species with highest number of identified sequences in the MiFish dataset at sample level and sorted by depth.

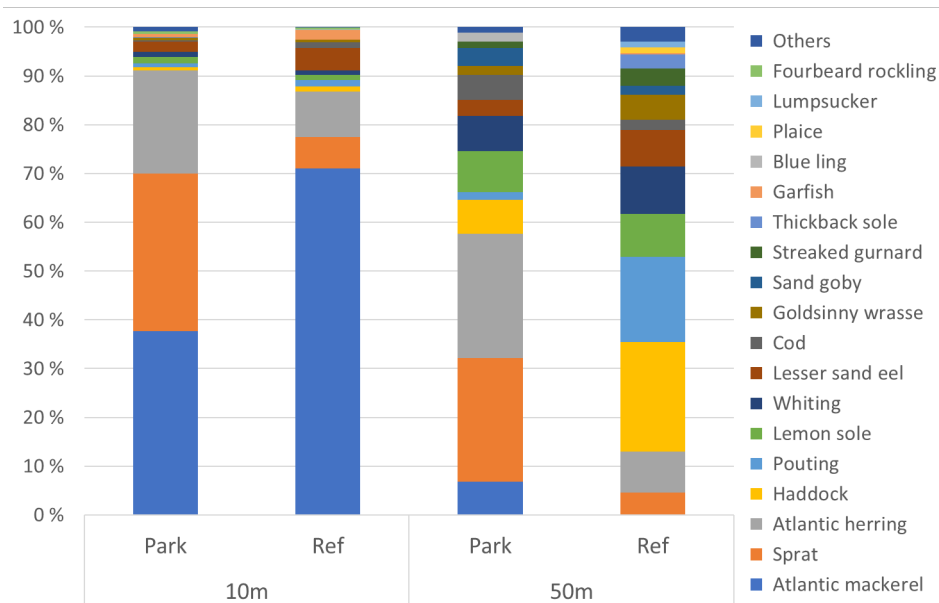


**Figure 12.** Comparison of relative abundance of the 18 species with highest number of identified sequences in the MiFish dataset at 10 and 50 m depth, and between wind farm and reference area.

**Table 3.** Absolute abundance of sequence reads for the top fish species as identified by the MitoFish database from the MiFish dataset, by depth including both farm and reference area.

Species	10m	50m	Species	10m	50m
Atlantic mackerel	873134	51575	Sand goby	9	41805
Sprat	380811	224977	Streaked gurnard	6	34248
Atlantic herring	284788	251808	Thickback sole	2046	20545
Haddock	13559	211917	Garfish	19763	1873
Pouting	16297	135808	Blue ling	1015	13861
Lemon sole	21993	126746	Plaice	5	8337
Whiting	16232	123812	Lumpsucker	1	8252
Lesser sand eel	53266	77677	Fourbeard rockling	7662	1
Cod	9786	53909	Others	9992	29878
Goldsinny wrasse	9374	50638			

**Table 4.** Absolute abundance of sequence reads for the top fish species as identified by the MitoFish database from the MiFish dataset, by farm and reference area. \* Indicate pelagic species.

Species	Park	Ref	Species	Park	Ref
Atlantic mackerel*	445483	479226	Sand goby	28437	13377
Sprat*	529598	76190	Streaked gurnard	9488	24766
Atlantic herring*	413565	123031	Thickback sole	1895	20696
Haddock	59446	166030	Garfish	6450	15186
Pouting	19543	132562	Blue ling	13861	1015
Lemon sole	78184	70555	Plaice	17	8325
Whiting	65513	74531	Lumpsucker	2	8251
Lesser sand eel	46370	84573	Fourbeard rockling	5227	2436
Cod	41300	22395	Others	17896	21974
Goldsinny wrasse	19696	40316			

The identified fish species included both the pelagic schooling mackerel, sprat and herring, and demersal species. Mackerel, sprat, and herring were more common in the 10 m samples than at 50 m, especially evident in the case of mackerel (Table 3; Fig. 12A) corroborating the results from ddPCR. Compared to the reference area, the farm had higher abundances of sprat and herring, with a lower abundance of mackerel (Table 4; Fig. 12B).

Pairwise similarities at OTU level between samples were calculated using the Bray-Curtis index with Hellinger-transformed data. The resultant similarities have been visualized using NMDS plots to show clustering of samples based on depth or farm vs. reference area (Fig. 13).

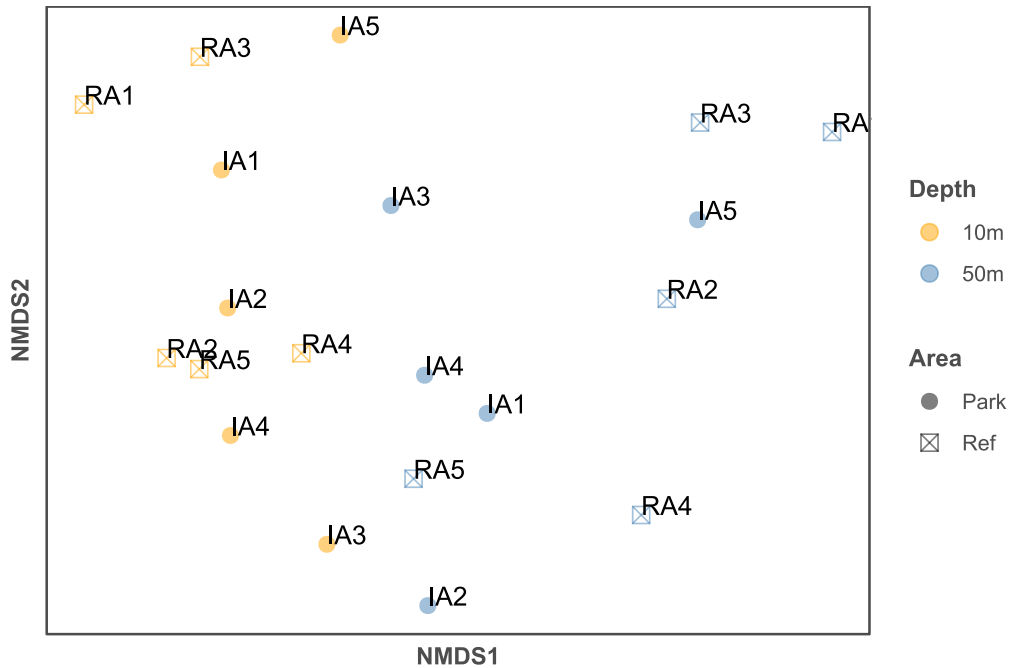


**Figure 13.** NMDS plot of Bray-Curtis pairwise similarity showing stations color coded by depth, and with symbols indicating farm or reference area.

The NMDS analysis revealed some evident clustering based on depth, but no clear pattern based on park vs. reference area. Average linkage clustering analysis of the same distance data showed initial separation between four 50 m stations, then another group of 50 m stations found clustered between two clusters of 10 m stations (Fig. 14).

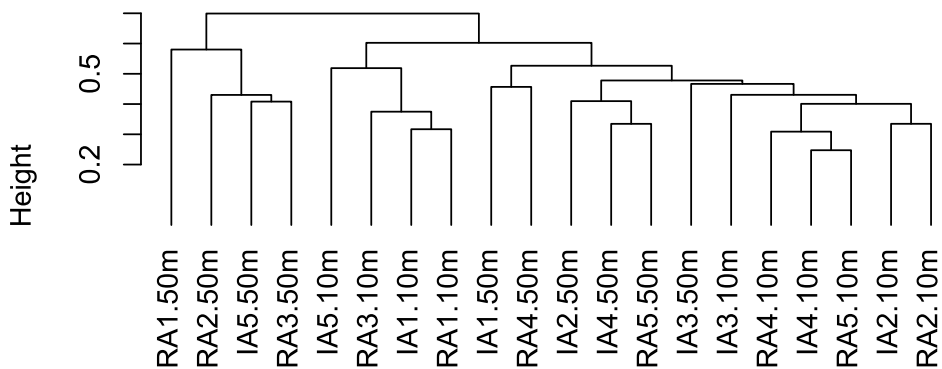


**Figure 14.** Average linkage cluster dendrogram from Bray-Curtis pairwise similarity of MiFish data showing degree of similarity between samples.

PERMANOVA analysis of the MiFish dataset showed significant differences for depth ( $F = 15.843$ ;  $p = 0.001$ ), and between park and reference area ( $F = 7.395$ ;  $p = 0.001$ ). SIMPER analysis showed that mackerel abundance accounted for close to 21% of the observed differences between samples, followed by Atlantic herring and sprat at 11% each, haddock at 10.5%, pouting at 7.5%, lemon sole 7%, whiting and lesser sand eel each 5% followed by all remaining species at slightly over 22% in total.

### 3.3. 18S rRNA metabarcoding results

For the 18S rRNA V1-V2 universal eukaryote dataset, the total number of raw sequences were 22 337 085 from 60 samples (five park and five reference stations, each at 10 and 50 m depth, each with three replicates) and 31 controls, with 45 828-827 730 sequences from individual samples (average: 337 268). After bioinformatic processing and filtering, 18 308 093 sequences remained. After SWARM clustering, 365 038 potential OTUs were identified from sequences in the dataset, with 3 598 OTUs were retained after chimera filtering and LULU curation. Taxonomic assignment of these OTUs after abundance filtering, using CREST4 with the SilvaMod 1.38 database, yielded 338 taxonomic groups at various level of resolution (Appendix A).

The most abundant taxon at kingdom level was the protist group Alveolata, containing, among others, dinoflagellates, and ciliates. The second most abundant kingdom was Metazoa, constituting all multicellular animals, third unassigned sequences, fourth Haptophyta algae and fifth the protist group Stramenopiles (Fig. 15). There was a slightly higher metazoan abundance at 10 m relative to 50 m in both wind farm and reference areas, but otherwise no clear differences between depth and area (Fig. 16).

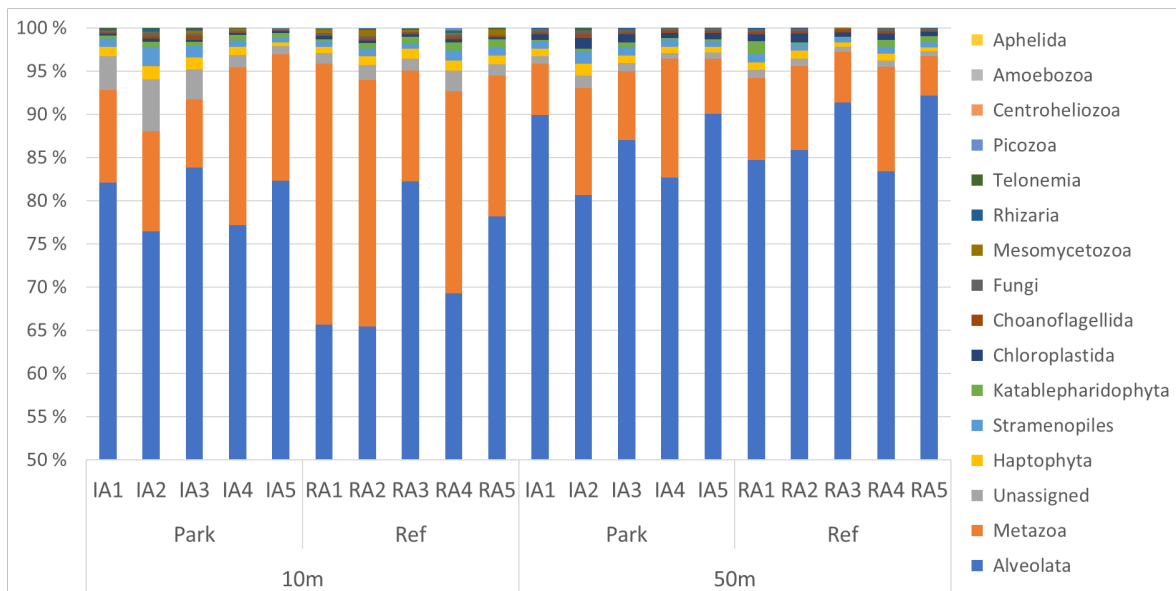


**Figure 15.** Relative abundance of the 16 taxa at kingdom level recovered in the 18S dataset. Due to the large abundance of Alveolata sequences, the y axis is scaled to the upper 50% to show less abundant taxa.

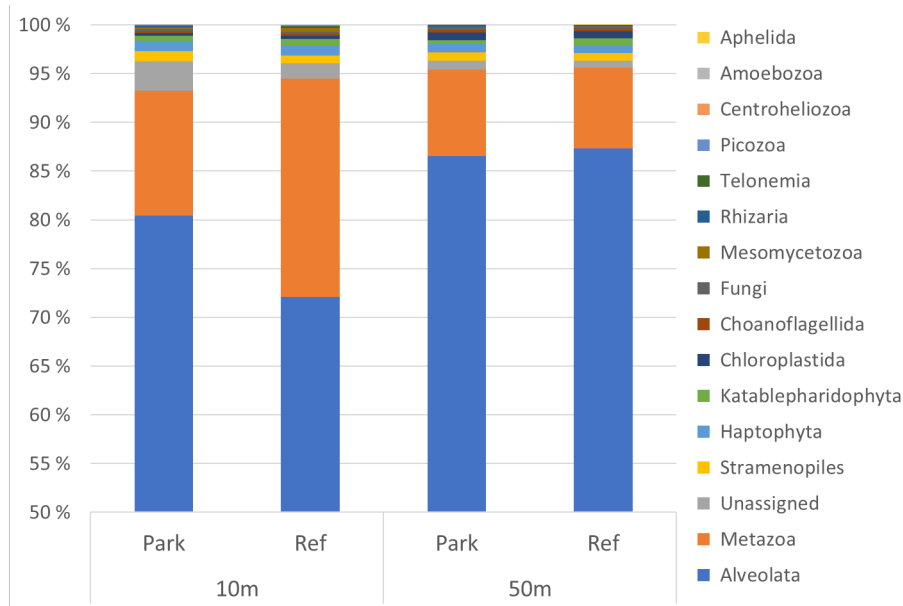


**Figure 16.** Comparison of relative abundance at kingdom level at 10 and 50 m depth, and between wind farm and reference area. Due to the large abundance of Alveolata sequences, the y axis is scaled to the upper 50% to show less abundant taxa.

Looking specifically at the metazoan kingdom (multicellular animals) only in the 18S dataset at the phylum level, the clearly most abundant phylum, with over 80-95% relative abundance between stations, was Arthropoda, due to the large number of calanoid sequences in the dataset, followed by cnidarians (jellyfish, anemones, and hydrozoans), unidentified metazoans and annelids (segmented worms), and Ctenophora (comb jellies) (Fig. 17).

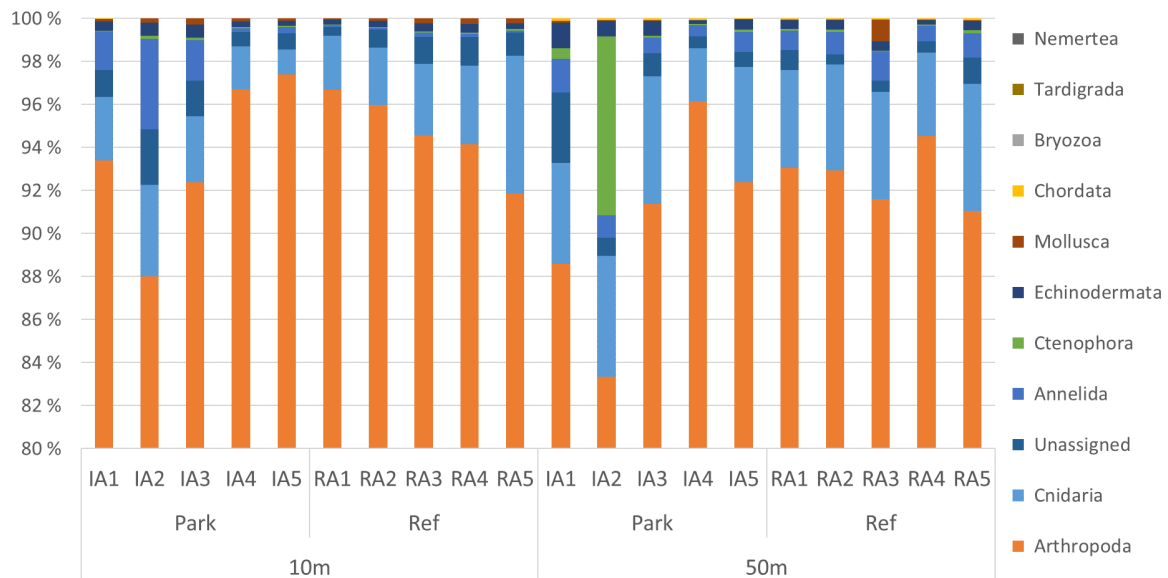


**Figure 17.** Metazoan relative abundance in the 18S rRNA dataset at phylum level. Due to the large abundance of Arthropoda sequences, the y axis is scaled to the upper 20% to show less abundant taxa.

Pairwise similarities between the OTU-level distributions at the different samples were calculated at OTU level using the Bray-Curtis index with Hellinger-transformed data. The resultant similarities

have been visualized using NMDS (non-metric multidimensional scaling) plots to show clustering of samples based on depth or farm vs. reference area (Fig. 18).



**Figure 18.** NMDS plot of Bray-Curtis pairwise similarity showing stations color coded by depth, and with symbols indicating farm or reference area.

The NMDS analysis demonstrated clear clustering based on depth. Three 10 m stations at the wind farm show a different composition from other 10 m stations, but no other clear pattern based on park or reference area was evident. A similar pattern was evident in the average linkage clustering analysis (Fig. 19).

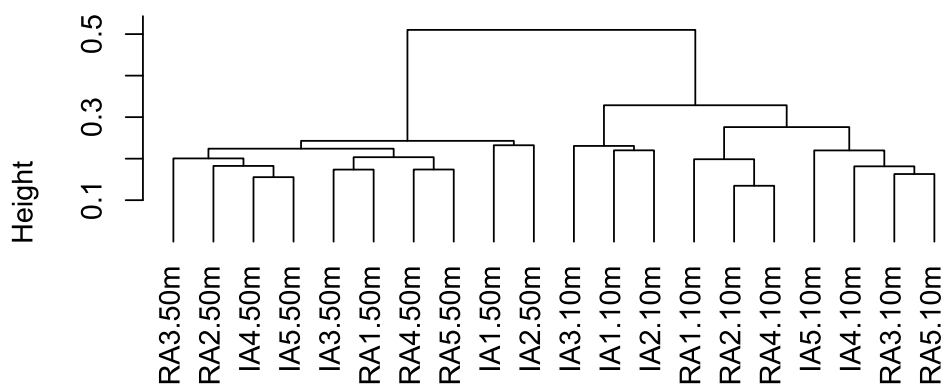


**Figure 19.** Average linkage cluster dendrogram from Bray-Curtis pairwise similarity of the 18S rRNA data showing degree of similarity between samples.

PERMANOVA analysis of the 18S rRNA dataset at OTU level showed clear significant differences due to depth ( $F = 101.047$ ;  $p = 0.001$ ), and significant differences between park and reference area ( $F = 7.261$ ;  $p = 0.003$ ). SIMPER analysis showed that dinoflagellate groups accounted for over 52% of the observed differences between samples, followed by Arthropoda (almost exclusively copepods) at



just over 20%, unidentified sequences a further 8.5%, followed by all remaining taxa at a collective 20%.

## 4. Discussion and conclusions

For a bit of context, and since no fish survey data are available for the area, we were able to obtain observational information about local fisheries catches in and around the Hywind wind park around the time of the pilot study water sampling campaign. Of relevance to this study is the timing of the main herring season, which normally occurs in June/July just before the commencement of spawning and lasts approximately 4 weeks. This suggests that in addition to fish, molecular detection results for herring might also originate from herring sperm, eggs or larvae if herring had recently returned to the Buchan Deep for spawning. For mackerel and sprat, there are no significant fisheries in the Hywind area, although this does not discount the possibility that considerable numbers of mackerel and/or sprat patrol the Hywind area in search of prey. We also learned that the Buchan Deep primarily comprises a seasonal haddock fishery for local Scottish fisherman. Since haddock is a demersal fish, our water sampling design is not optimal for detection of such bottom-dwelling fish (although see Results and Discussion for occurrence of haddock in the metabarcoding data).

### 4.1. Droplet digital PCR

Quantitative molecular analysis of two keystone pelagic fish species in the North Sea, Atlantic mackerel (*Scomber scombrus*) and Atlantic herring (*Clupea harengus*) demonstrated species-specific patterns of eDNA detection in the Hywind wind park compared to the adjacent reference area. Additionally, our observation of non-homogeneous vertical eDNA distribution in the water column (maximum depth approx. 100 m) suggests that the optimal depth for water sampling in eDNA-based pelagic fish surveys may vary in areas with vertical stratification (Closek et al. 2019; Jeunen et al. 2020). Alternatively, the spatial and vertical distribution of degradation-prone eDNA may be anecdotal to some degree as schools of pelagic fish are constantly moving through the water column, in which case the single water sampling events conducted at each station during the field campaign are representative only as “snapshots” of local fish activity (Yamamoto et al. 2016).

One persistent challenge with the development of eDNA-based studies for application within a regulatory framework for fisheries management is the unclear relationship between eDNA signal and biomass (Rourke et al. 2022). Although the ddPCR results from this pilot study do not permit estimation of biomass, we did take the opportunity to compare the absolute detected quantities of mackerel and herring eDNA (ddPCR results) with the relative abundance of both species in the MiFish metabarcoding results (Fig. 20). Both mackerel (Fig. 20A) and herring (Fig. 20B) were detected using ddPCR and MiFish metabarcoding, and linear regression for each species indicates significant, albeit weak positive correlations between the two methods. The low strength of these correlations is likely due, in part, to non-detections for both sets of results. In general, however, these regressions support an agreement between the two methods and lend modest support toward semi-qualitative interpretation of metabarcoding results.

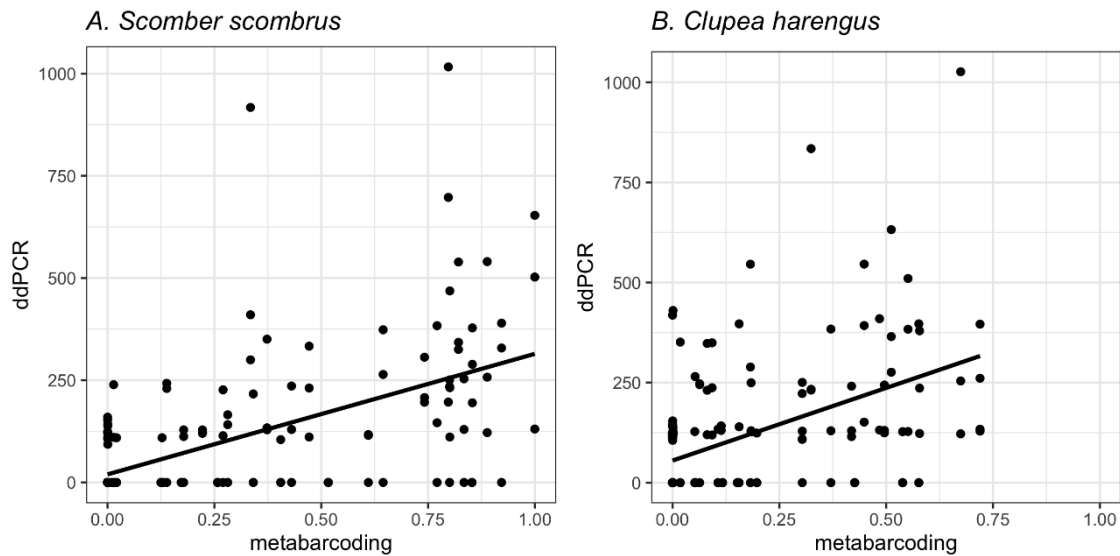


**Figure 20.** Comparison of metabarcoding and ddPCR results for (A) Atlantic mackerel and (B) Atlantic herring. Relative abundance of mackerel or herring reads in metabarcoding libraries is shown on the x-axis, while ddPCR target gene copies per liter of seawater is shown on the y-axis. Non-detections were arbitrarily set to 0 for visualization purposes.

Our sampling method using triplicate one-liter water samples is aligned with multiple contemporary eDNA-based fish studies that aimed to find the best compromise between sample concentration and acquisition feasibility (Capo et al. 2020 and references therein). Despite this, the ddPCR results generated in this study were near the limit of detection for the ddPCR instrument, raising questions about true versus false positive detections (Hunter et al. 2017). While requiring a longer filtration time, more consistent results (i.e. lower limit of detection) may have been achieved by a larger sample volume. As the ddPCR assays used were obtained from a published study which reported rigorous optimization and specificity testing (Knudsen et al. 2019), we have no reason to suspect poor performance of the assay itself. Full validation of the assays applied and calculation of their reliable limits of detection on the ddPCR platform (Klymus et al. 2020) and with relevant levels of potential PCR inhibitors (Hunter et al. 2019), however, falls outside the scope of this pilot study.

Without the ability to compare our ddPCR detection results with other survey methods conducted at the same time (Knudsen et al. 2019), our eDNA results can only be indicative for relative abundance between the two sampled areas rather than conclusive of actual biomass present in the samples areas.

## 4.2. Metabarcoding

The 12S MiFish marker dataset identified 39 different fish species, including a variety of pelagic and demersal species, with demersal species generally being more common at 50 m than at the shallower 10 m samples. The highest metabarcoding abundances were identified as commercially important pelagic schooling species such as mackerel, sprat, and herring. Mackerel abundance was much higher at 10 m depth than at 50 m depth, while sprat was more abundant in the park area at both depths compared to the reference areas. For both fish species, without a higher sampling frequency over time and season, such abundance variability should be considered a measure of

placement of schools at that time. However, the results suggest that the method can detect differences in abundance of these species.

Man-made structures create a fish aggregation device (FAD) effect in that many fish species, for various reasons, tend to congregate around objects in the sea (Bergström et al. 2013), and wind farms have been shown to harbor high fish abundance (Methratta et al. 2019). While this serves as a possible explanation for the observed higher MiFish sequence read abundance of sprat and herring in the wind farm area, it might equally well be a result of other effects or random placement of schools at the time of the survey: pelagic fish are highly dynamic in time and space (Lindeboom et al. 2011), and any farm vs. reference area trend would have to be backed up by multiple time points beyond the scope of this pilot study.

MiFish primers are designed to be universal across fish species, but this does not preclude primer bias, i.e., that certain species have higher or lower read abundance than actual presence in the sampling area. As we did not do a direct comparison with data from morphological surveys, we could not readily identify any species gaps in the metabarcoding coverage here. Another caveat is that correct taxonomic identification of fish species is dependent on the closest species represented in the taxonomic database used, here the MitoFish database; misattribution to closely related species is possible.

In addition to fish species described above, the MiFish dataset also included non-target sequences identified as human, cattle (*Bos taurus*) and sheep (*Ovis aries*). These sequences were found throughout the dataset, and not specifically in control samples. While no rigorous study on their origin was done here, a possible explanation for these sequences could include human impact on the marine environment through for instance sewage or ship activity. Interestingly, an additional non-target species that was detected in the MiFish dataset was harbor porpoise, albeit with very low abundance. This species may be underreported in terms of abundance given the potential for primer bias against this species, however. While porpoises are known to shy away from wind farm construction activity, Scheidat et al. found no adverse impact during the operational phase (2011).

Supplementing the MiFish results, the 18S rRNA V1-V2 marker provides a contrasting view into the wider diversity of multicellular and single-cell non-bacterial organisms in the water column. Due to the complexity of the dataset, it is shown here at kingdom and phylum level, meaning individual taxa are less immediately visible. In the clustering analyses, 18S dataset beta diversity shows a clear separation between 10 and 50 m depth across the dataset. This confirms the ability of the 18S metabarcoding data to discriminate between organism communities at different layers and validates the ability to pick up changes in eukaryote communities based on changes in environmental conditions. No clear pattern emerged for differences between farm and reference areas, however, though three 10 m samples from the wind farm were a bit less like other stations both from farm and reference areas. A closer look would include more in-depth analysis of specific OTUs identified not part of the scope here.

In conclusion, both MiFish and 18S metabarcoding datasets were able to demonstrate significant differences between 10 and 50 m samples, highlighting the utility of metabarcoding data in representing changes in organism community composition due to depth. The range of identified fish species shows that MiFish metabarcoding data can detect and provide rough abundance estimates of fish species composition in the water, highlighting the applicability of the method for future monitoring surveys. The relative simplicity of the MiFish data also aids interpretation of

metabarcoding results. Yet differences in composition between farm and reference areas should be treated with caution: There was no consistent clustering of farm or reference stations within 10 and 50 m datasets for either MiFish or 18S data (Fig. 14, 19), and differences in e.g., pelagic fish and other abundances might also be due to other or random factors that cannot be thoroughly examined from a single point alone. Thus, as a pilot study, these results successfully show that metabarcoding can be used as an attractive supplement to existing study methodology, though, like for other methods, a more comprehensive monitoring regime would be necessary to establish consistent trends in organism composition inside and outside the wind farm.

## 5. References

- Bergström, L., Sundqvist, F., Bergström, U., 2013. Effects of an offshore wind farm on temporal and spatial patterns in the demersal fish community. *Mar. Ecol. Prog. Ser.* 485, 199–210. <https://doi.org/10.3354/meps10344>
- Bergström, L., Kautsky, L., Malm, T., Rosenberg, R., Wahlberg, M., Åstrand Capetillo, N., Wilhelmsson, D., 2014. Effects of offshore wind farms on marine wildlife—a generalized impact assessment. *Environ. Res. Lett.* 9, 034012. <https://doi.org/10.1088/1748-9326/9/3/034012>
- Capo, E., Spong, G., Königsson, H. and Byström, P., 2020. Effects of filtration methods and water volume on the quantification of brown trout (*Salmo trutta*) and Arctic char (*Salvelinus alpinus*) eDNA concentrations via droplet digital PCR. *Environmental DNA* 2, 152-160. <https://doi.org/10.1002/edn3.52>
- Chamberlain, S. and Sagouis, A. 2021. parzer: Parse Messy Geographic Coordinates. R package version 0.4.1. <https://CRAN.R-project.org/package=parzer>
- Dempster, T., Taquet, M., 2004. Fish aggregation device (FAD) research: gaps in current knowledge and future directions for ecological studies. *Rev Fish Biol Fisheries* 14, 21–42. <https://doi.org/10.1007/s11160-004-3151-x>
- Hunter, M.E., Dorazio, R.M., Butterfield, J.S., Meigs-Friend, G., Nico, L.G. and Ferrante, J.A., 2017. Detection limits of quantitative and digital PCR assays and their influence in presence–absence surveys of environmental DNA. *Molecular ecology resources*, 17(2), pp.221-229. <https://doi.org/10.1111/1755-0998.12619>
- Hunter, M.E., Ferrante, J.A., Meigs-Friend, G. and Ulmer, A., 2019. Improving eDNA yield and inhibitor reduction through increased water volumes and multi-filter isolation techniques. *Scientific Reports* 9, 1-9. <https://doi.org/10.1038/s41598-019-40977-w>
- Inger, R., Attrill, M.J., Bearhop, S., Broderick, A.C., James Grecian, W., Hodgson, D.J., Mills, C., Sheehan, E., Votier, S.C., Witt, M.J., Godley, B.J., 2009. Marine renewable energy: potential benefits to biodiversity? An urgent call for research. *Journal of Applied Ecology*. <https://doi.org/10.1111/j.1365-2664.2009.01697.x>
- Ivanov, E., Capet, A., De Borger, E., Degraer, S., Delhez, E.J.M., Soetaert, K., Vanaverbeke, J., Grégoire, M., 2021. Offshore Wind Farm Footprint on Organic and Mineral Particle Flux to the Bottom. *Front. Mar. Sci.* 8, 631799. <https://doi.org/10.3389/fmars.2021.631799>
- Jeunen, G.J., Lamare, M.D., Knapp, M., Spencer, H.G., Taylor, H.R., Stat, M., Bunce, M. and Gemmell, N.J., 2020. Water stratification in the marine biome restricts vertical environmental DNA (eDNA) signal dispersal. *Environmental DNA* 2, 99-111. <https://doi.org/10.1002/edn3.49>
- Klymus, K.E., Merkes, C.M., Allison, M.J., Goldberg, C.S., Helbing, C.C., Hunter, M.E., Jackson, C.A., Lance, R.F., Mangan, A.M., Monroe, E.M. and Piaggio, A.J., 2020. Reporting the limits of detection and quantification for environmental DNA assays. *Environmental DNA* 2, 271-282. <https://doi.org/10.1002/edn3.29>

Knudsen, S.W., Ebert, R.B., Hesselsøe, M., Kuntke, F., Hassingboe, J., Mortensen, P.B., Thomsen, P.F., Sigsgaard, E.E., Hansen, B.K., Nielsen, E.E. and Møller, P.R., 2019. Species-specific detection and quantification of environmental DNA from marine fishes in the Baltic Sea. *Journal of experimental marine biology and ecology*, 510, pp.31-45.

<https://doi.org/10.1016/j.jembe.2018.09.004>

Lindeboom, Han J.; H. J. Kouwenhoven; M. J. N. Bergman; S. Bouma; S. Brasseur; R. Daan; R. C. Fijn; D. de Haan; S. Dirksen; R. van Hal; R. Hille Ris Lambers; Remmentter Hofstede; K. L. Krijgsveld; M. Leopold and M. Scheidat 2011 “Short-term ecological effects of an offshore wind farm in the Dutch coastal zone; a compilation”, *Environmental Research Letters* 6(3): 1-13.

<https://doi.org/10.1088/1748-9326/6/2/025102>

Methratta, Elizabeth T. and William R. Dardick 2019 “Meta-Analysis of Finfish Abundance at Offshore Wind Farms”, *Reviews in Fisheries Science & Aquaculture* 27(2): 242–260.

<https://doi.org/10.1080/23308249.2019.1584601>

Methratta, E.T., 2021. Distance-Based Sampling Methods for Assessing the Ecological Effects of Offshore Wind Farms: Synthesis and Application to Fisheries Resource Studies. *Front. Mar. Sci.* 8, 674594. <https://doi.org/10.3389/fmars.2021.674594>

Monuki, K., Barber, P.H. and Gold, Z., 2021. eDNA captures depth partitioning in a kelp forest ecosystem. *PloS one* 16, p.e0253104. <https://doi.org/10.1371/journal.pone.0253104>

Munnelly, R.T., Reeves, D.B., Chesney, E.J., Baltz, D.M., 2021. Spatial and Temporal Influences of Nearshore Hydrography on Fish Assemblages Associated with Energy Platforms in the Northern Gulf of Mexico. *Estuaries and Coasts* 44, 269–285. <https://doi.org/10.1007/s12237-020-00772-7>

R Core Team. 2021. R: A language and environment for statistical computing. R Foundation for Statistical Computing. Vienna, Austria. <https://www.R-project.org/>

Rourke, M.L., Fowler, A.M., Hughes, J.M., Broadhurst, M.K., DiBattista, J.D., Fielder, S., Wilkes Walburn, J. and Furlan, E.M., 2022. Environmental DNA (eDNA) as a tool for assessing fish biomass: A review of approaches and future considerations for resource surveys. *Environmental DNA* 4, 9-33. <https://doi.org/10.1002/edn3.185>

Scheidat, M., Tougaard, J., Brasseur, S., Carstensen, J., van Polanen Petel, T., Teilmann, J., & Reijnders, P., 2011. Harbour porpoises (*Phocoena phocoena*) and wind farms: a case study in the Dutch North Sea. *Environmental Research Letters*, 6(2), 025102. <http://doi.org/10.1088/1748-9326/6/2/025102>

Shelton, A.O., Ramón-Laca, A., Wells, A., Clemons, J., Chu, D., Feist, B.E., Kelly, R.P., Parker-Stetter, S.L., Thomas, R., Nichols, K.M., Park, L., 2022. Environmental DNA provides quantitative estimates of Pacific hake abundance and distribution in the open ocean. *Proc. R. Soc. B.* 289, 20212613. <https://doi.org/10.1098/rspb.2021.2613>

Slavik, K., Lemmen, C., Zhang, W., Kerimoglu, O., Klingbeil, K., Wirtz, K.W., 2019. The large-scale impact of offshore wind farm structures on pelagic primary productivity in the southern North Sea. *Hydrobiologia* 845, 35–53. <https://doi.org/10.1007/s10750-018-3653-5>

Stoeckle, M.Y., Adolf, J., Charlop-Powers, Z., Dunton, K.J., Hinks, G., VanMorter, S.M., 2021. Trawl and eDNA assessment of marine fish diversity, seasonality, and relative abundance in coastal New Jersey, USA. *ICES Journal of Marine Science* 78, 293–304. <https://doi.org/10.1093/icesjms/fsaa225>

Sumer, B., and J. Fredsøe. 1997. *Hydrodynamics around Cylindrical Structures*. World Scientific, Singapore.

van Berkel, J., Burchard, H., Christensen, A., Mortensen, L., Petersen, O., Thomsen, F., 2020. The Effects of Offshore Wind Farms on Hydrodynamics and Implications for Fishes. *Oceanog* 33, 108–117. <https://doi.org/10.5670/oceanog.2020.410>

Wickham, H. 2016. *ggplot2: Elegant Graphics for Data Analysis*. New York: Springer-Verlag. ISBN 978-3-319-24277-4. <https://ggplot2.tidyverse.org>

Yamamoto, S., Minami, K., Fukaya, K., Takahashi, K., Sawada, H., Murakami, H., Tsuji, S., Hashizume, H., Kubonaga, S., Horiuchi, T. and Hongo, M., 2016. Environmental DNA as a ‘snapshot’ of fish distribution: A case study of Japanese jack mackerel in Maizuru Bay, Sea of Japan. *PloS one* 11, e0149786. <https://doi.org/10.1371/journal.pone.0149786>

Acknowledgements: The authors thank Equinor for collaboration and support to conduct this study, in particular Kari Mette Murvoll, Ane Kjølhamar and Anita Skarstad. Equinor was represented in Peterhead by Ben Lawson, Peter Massie and Euan Rogerson. Additional help in Peterhead was provided by Brown & May Marine Ltd. The fieldwork was conducted during one day aboard the “MCS Swath 1” where the captain and crew are thanked. Ian Todd and co-workers Sophie Cox and Alexandra Hiley at Ocean Science Consulting Limited (OSC), provided necessary equipment and assistance at sea.





**Appendix B, Figure 1.** *Total read abundances for the MiFish dataset with taxonomic assignments listed as common names. Names with an asterisk identified through blastn database rather than MitoFish, and represent non-target (i.e., non-fish) species.*